Supporting Information

Structural and Permeation Kinetic Correlations in PdCuAg Membranes

Lingfang Zhao, Andreas Goldbach, Chun Bao, Hengyong Xu*

Dalian National Laboratory for Clean Energy, Dalian Institute of Chemical Physics, Chinese Academy of Sciences, 457 Zhongshan Road, 116023 Dalian, China

Corresponding Author

*E-mail: goldbach@dicp.ac.cn.

phone: + 86 411 8437 9229; fax +86 411 8469 1570.

Leak flow correction of H_2 permeation data

The most important gas transport modes through porous layers are Knudsen diffusion (small pores) and viscous flow (large pores). Following Burggraaf and co-workers[1] the contribution of these flow regimes to an overall defect permeation rate can be derived from leak flow measurements according to

$$\Phi = \Phi_K + \Phi_v P_{mean} \quad \text{(S1)}$$

where Φ is the total gas permeability, Φ_K and Φ_v are the permeability due to Knudsen diffusion and viscous flow, respectively, and $P_{mean} = (P_{feed} + P_{perm})/2$ is the mean value of the feed and permeate side partial pressures. For a given porous layer Φ_K and Φ_v vary only with gas and temperature:

$$\Phi_K = \left(\frac{4\sqrt{2}\varepsilon r}{3\tau d\sqrt{\pi R}}\right)\frac{1}{\sqrt{MT}}, \quad \text{(S2)}$$

$$\Phi_v = \left(\frac{\varepsilon r^2}{8\tau R d}\right)\frac{1}{\eta T}, \quad \text{(S3)}$$

where ε is the porosity, τ tortuosity, r pore radius and d thickness of the porous layer, M molecular mass and η viscosity of the gas, and R the universal gas constant. According to Equation S1 a plot of Φ versus P_{mean} will be linear yielding Φ_K (abscissa intercept) and Φ_v (slope). Figure S1 shows final N_2 leak flows of membranes M1-M6 as function of temperature and pressure.

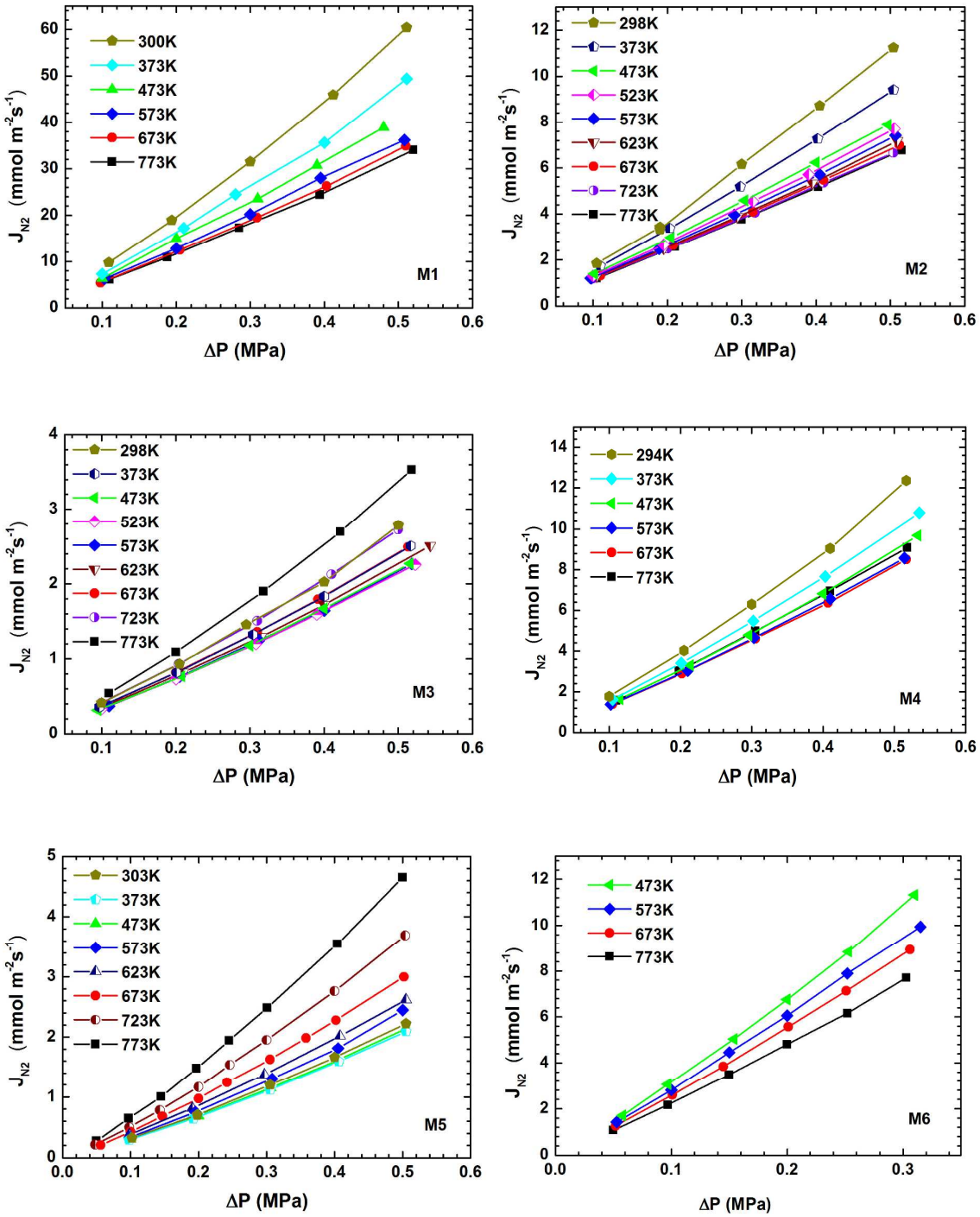

Figure S1. Final N_2 leak flows of membranes M1-M6 as function of temperature and pressure.

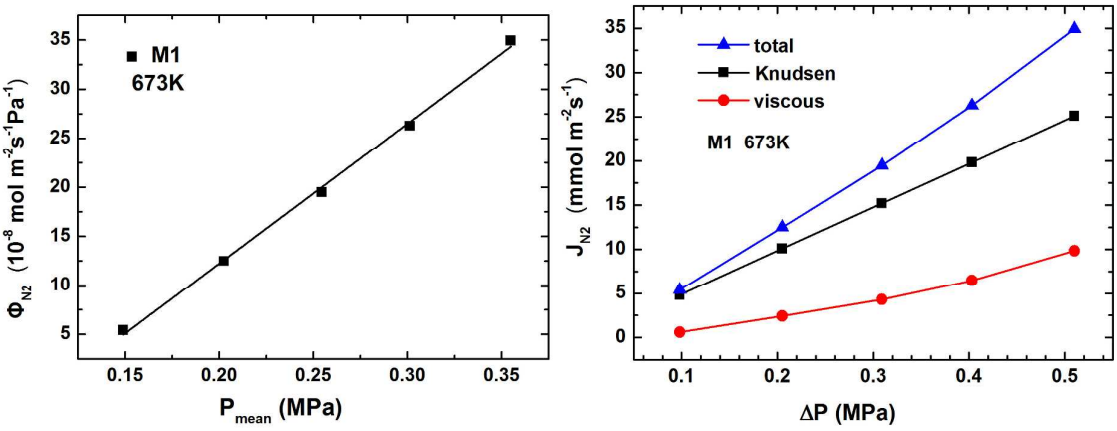

Figure S2. Dependence of M1 N_2 permeability at 673 K on mean pressure (left) and corresponding Knudsen and viscous flow components of that leak rate.

Table S1. Knudsen and viscous permeability components of N_2 and H_2 leak flows at 673 K and activation energies before (orig) and after correction for leak flow (Lcor) and correction for leak flow and support resistance (LScor).

membrane	$\Phi_{K,N2}$	$\Phi_{K,H2}$	$\Phi_{v,N2}$	$\Phi_{v,H2}$	$E_{act,\ orig}$	$E_{act,\ Lcor}$	$E_{act,\ LScor}$
	10^{-9} mol m^{-2} s^{-1} Pa^{-1}		10^{-15} mol m^{-2} s^{-1} Pa^{-2}		kJ mol^{-1}		
M1	49.2	184	54.1	109	7.5	8.6	8.8
M2	11.1	41.6	7.18	14.4	9.7	10.0	10.2
M3	3.08	11.5	5.03	10.1	19.3	19.5	19.8
M4	11.6	43.5	13.4	26.9	11.8	12.2	12.5
M5	3.46	12.9	7.28	14.6	11.9	12.3	12.6
M6	20.9	78.1	33.2	66.7	19.2	21.8	22.0

Figure S2 shows the linear regression analysis of the M1 leak rate at 673 K as an example (left). Such analyses were carried out for all data displayed in Figure S1. N_2 Knudsen and viscous permeability components $\Phi_{K,N2}$ and $\Phi_{v,N2}$ derived from the 673 K leaks flows are summarized for all membranes in Table S1 and the according Knudsen and viscous flow

components of M1 are shown in Figure S2 (right) for example. The corresponding H_2 Knudsen and viscous permeability components $\Phi_{K,H2}$ and $\Phi_{v,H2}$ and H_2 leak flow rate were calculated by rescaling coefficients $\Phi_{K,N2}$ and $\Phi_{v,N2}$ with $\sqrt{M_{N2}/M_{H2}}$ and η_{N2}/η_{H2}, respectively, for each membrane at each temperature employing tabulated gas viscosities.[2] The resulting $\Phi_{K,H2}$ and $\Phi_{v,H2}$ permeability values at 673 K are also included in Table S1 for example. Finally, H_2 leak flows were calculated with the help of these H_2 Knudsen and viscous permeabilities and subtracted from the experimental H_2 fluxes. Figure S3 compares the leak flow corrected with uncorrected permeation data showing that this correction was significant only for membrane M1 with the lowest selectivity (47) and membrane M6 with the lowest permeability. The leak flow correction was negligible for the membranes with high selectivity (> 600, M3 and M5) and high permeability (M4). Table S1 compares activation energies E_{act} derived from uncorrected and leak flow corrected H_2 fluxes demonstrating that the effect on the permeation kinetic parameters was also marginal there with exception of membranes M1 and M6.

Correction of H_2 permeation data for support transport resistance

The influence of support transport resistance on the measured H_2 permeation rates can be also determined with the help of Equations S1-S3. Permeability is defined as reciprocal resistance against mass transport through a (porous) medium.[3] A multilayer system can be considered as resistances in series,[3] so that permeability of such a system is given by

$$\Phi = \left(\sum_i \frac{1}{\Phi_i} \right)^{-1}, \qquad \text{(S4)}$$

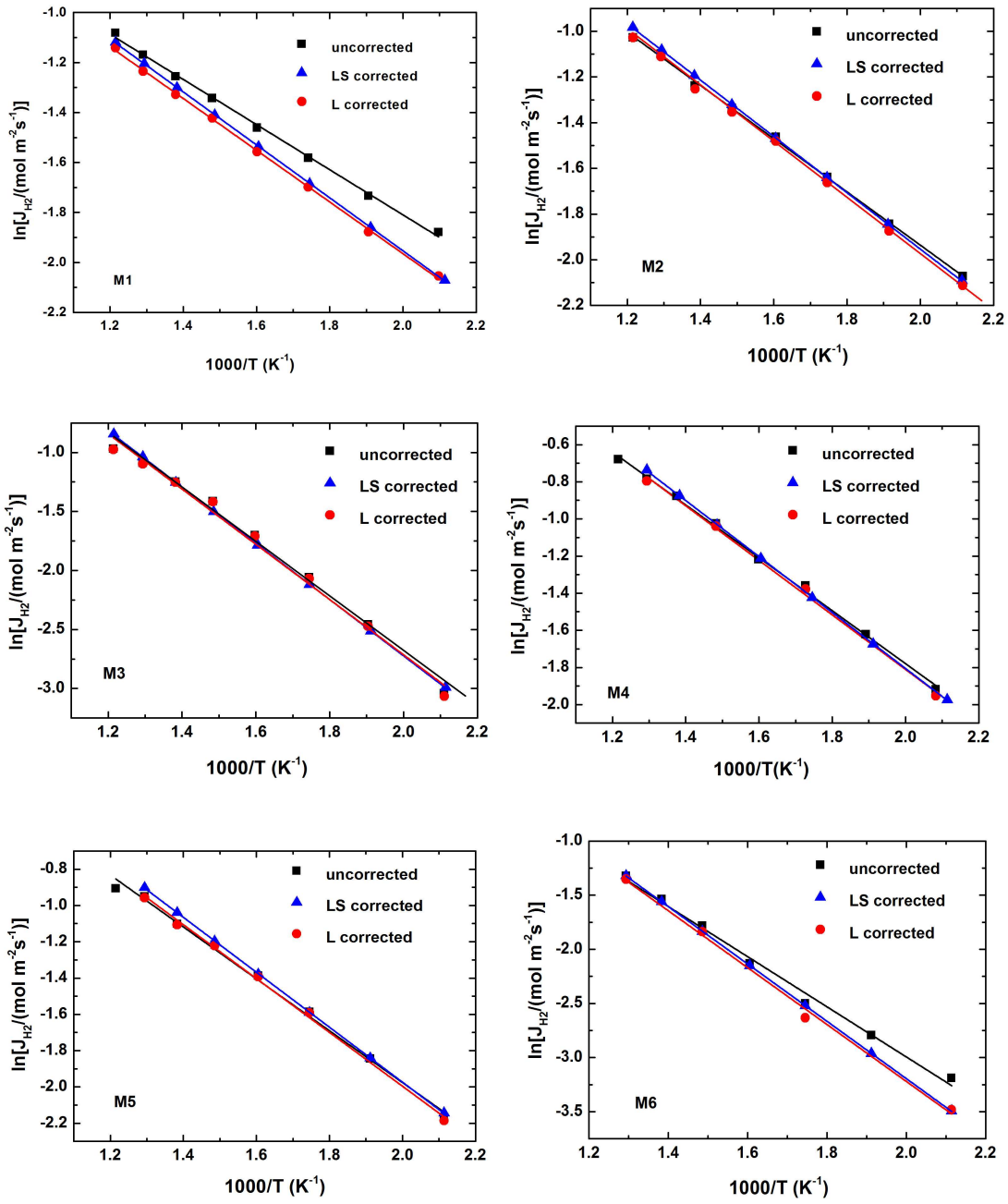

Figure S3. Hydrogen fluxes of membranes M1-M6 as measured (squares), after correction for leak flow contributions (circles, L corrected), and after correction for leak flow contributions plus support resistance influence (triangles, LS corrected).

where Φ_i is the permeability of layer *i*. The mass transport resistance of palladium composite membranes with the here employed ceramic substrates has been previously evaluated at 673 K showing that it is negligible (< 3%).[4] The tubular ceramic substrate consists of a 2 mm thick α-Al_2O_3 backbone with 43% porosity and 3.4 μm mean pore size (α_1 layer) and an approximately 80 μm thick α-Al_2O_3 double layer with 35% porosity and 160 nm mean pore size (α_2 layer).[4] The tortuosity is 1.25 for both layer types.[4] Thus, the permeability of the PdCuAg composite membranes is given by

$$\Phi = \left(\frac{1}{\Phi_{PdCuAg}} + \frac{1}{\Phi_{\alpha 2}} + \frac{1}{\Phi_{\alpha 1}} \right)^{-1} . \qquad \text{(S5)}$$

where Φ_{PdCuAg} denotes the intrinsic permeability of the PdCuAg layers. Table S2 shows that mean free path length λ of H_2 increases from 171 nm at 473 K to 280 nm at 773 K and 100 kPa (permeate side pressure). Hence, mass transport through the ceramic backbone is governed by viscous flow while that through the intermediate double layer is dominated by Knudsen diffusion. The calculated permeability of the support layers cannot be directly used for determination of Φ_{PdCuAg} because of differing pressure units, i.e. Pa^{-1} for $\Phi_{\alpha 1}$ and $\Phi_{\alpha 2}$ vs. ~~Pa$^{-0.6-0.65}$~~ for Φ. Hence we have calculated H_2 permeation rates $J_{\alpha 1}$ and $J_{\alpha 2}$ for both ceramic layers at ΔP = 100 kPa for each experimental temperature which are listed in Table S2. These have been used to determine intrinsic H_2 permeation rates J_{PdCuAg} from leak flow corrected experimental permeation rates J_{H2} at ΔP = 100 kPa according to

$$J_{PdCuAg} = \left(\frac{1}{J_{H2}} + \frac{1}{J_{\alpha 2}} + \frac{1}{J_{\alpha 1}} \right)^{-1} . \qquad \text{(S5)}$$

Table S2 lists both J_{H2} and J_{PdCuAg} for membrane M6 as well as the deviation ΔJ_{H2} between both permeation rates as function of temperature for example. In addition Figure S3 depicts the leak flow plus support resistance corrected H_2 permeation rates for all membranes demonstrating that mass transport resistance of the support reduces the intrinsic H_2 permeation rates of the PdCuAg alloy layers minimally under our experimental conditions. The effect of support resistance on the permeation kinetic parameters is also marginal as shown by the activation energies derived from H_2 permeation rates corrected for leak flow and support resistance (Table S1).

Table S2. Intrinsic H_2 permeation rates of M6 PdCuAg alloy, intermediate α-Al_2O_3 double layer (α2) and α-Al_2O_3 support backbone (α1) at ΔP = 100 kPa.

T	λ	J_{H2}	$J_{\alpha 1}$	$J_{\alpha 2}$	J_{PdCuAg}	ΔJ_{H2}
K	nm		mol m^{-2} s^{-1}			%
473	171	0.030	101.	24.8	0.030	0.2
523	189	0.052	88.1	23.2	0.052	0.3
573	207	0.080	78.0	21.9	0.080	0.5
623	225	0.115	69.9	20.8	0.116	0.7
673	243	0.158	63.3	19.8	0.159	1.0
723	261	0.206	57.8	19.0	0.209	1.4
773	280	0.261	53.2	18.2	0.266	1.9

Structure-function correlations

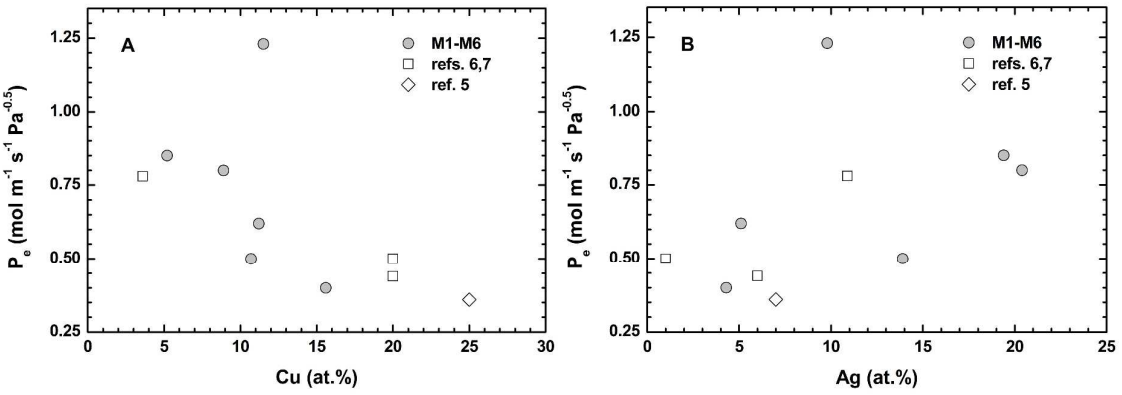

Figure S4. Interdependence between H_2 permeability P_e at 673 K and (A) copper and (B) silver content of PdCuAg membranes. Note the decreasing and increasing trends of P_e with increasing Cu and Ag content, respectively.

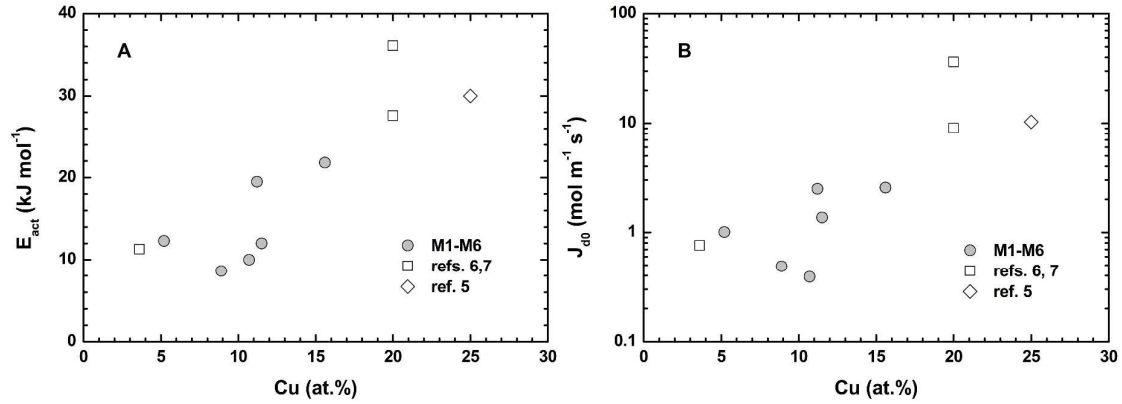

Figure S5. Interdependence between copper content of PdCuAg membranes and (A) activation energy E_{act} and (B) pre-exponential factor J_{d0} of H_2 permeation laws. Note the increasing trends of both quantities with increasing copper content.

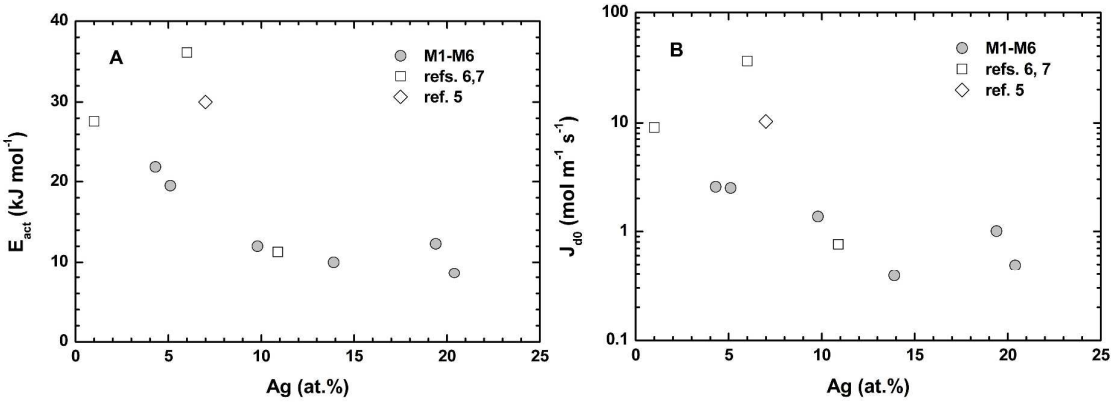

Figure S6. Interdependence between silver content of PdCuAg membranes and (A) activation energy E_{act} and (B) pre-exponential factor J_{d0} of H_2 permeation laws. Note the decreasing trends of both quantities with increasing silver content.

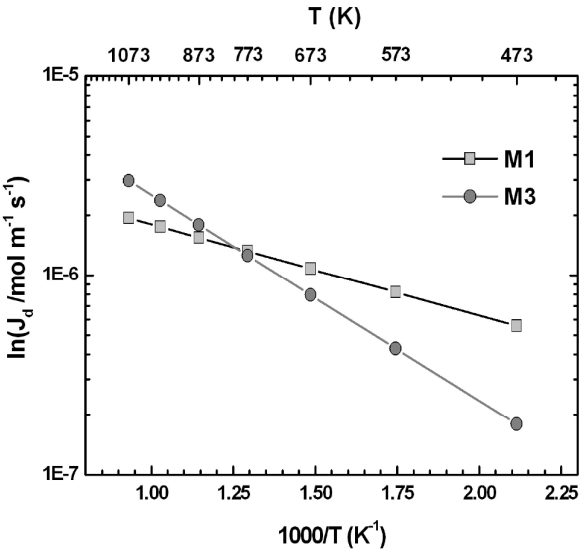

Figure S7. H_2 permeation rates of Ag-rich membrane M1 with E_{act} = 8.8 kJ mol^{-1} and Cu-rich membrane M3 with E_{act} = 19.8 kJ mol^{-1} normalized to PdCuAg layer thickness. Note that the Ag-rich membrane exhibits higher H_2 permeation rates below the isokinetic point around 800 K but lower permeation rates than the Cu-rich membrane above that temperature.

References

(1) Keizer, K., Uhlhorn, R. J. R., Van vuren, R. J., Burggraaf, A. J. Gas Separation Mechanisms in Microporous Modified Gamma Alumina Membranes. *J. Membr. Sci.* **1988**, *39*, 285-300.

(2) http://www.lmnoeng.com/Flow/GasViscosity.htm.

(3) Uhlhorn, R. J. R., Keizer, K., R. J., Burggraaf, A. J. Gas and Surface Diffusion in Modified γ-Alumina Systems. *J. Membr. Sci.* **1989**, *46*, 225-241.

(4) Boon, J.; Pieterse, J. A. Z.; Dijkstra, J. W., van Sint Annaland, M. Modelling and Systematic Experimental Investigation of Mass Transfer in Supported Palladium-Based Membrane Separators.

(5) Tarditi, A. M.; Braun, F.; Cornaglia, L. M. Novel PdAgCu Ternary Alloy: Hydrogen Permeation and Surface Properties. *Appl. Surf. Sci.* **2011**, *257*, 6626-6635.

(6) Peters, T. A.; Kaleta, T.; Stange, M.; Bredesen, R. Development of Thin Binary and Ternary Pd-Based Alloy Membranes for Use in Hydrogen Production. *J. Membr. Sci.* **2011**, *383*, 124-134.

(7) Peters, T. A.; Kaleta, T.; Stange, M.; Bredesen, R. Development of Ternary Pd-Ag-TM Alloy Membranes with Improved Sulphur Tolerance. *J. Membr. Sci.* **2013**, *429*, 448-458.